Proceedings XXI GEOINFO, November 30 - December 03, 2020, São José dos Campos, SP, Brazil. p 106-117

Circular Hough Transform and Balanced Random Forest to Detect Center Pivots

Marcos L. Rodrigues[1], **Thales S. Körting**[1], **Gilberto R. De Queiroz**[1]

[1]National Institute for Space Research (INPE)
Caixa Postal 515 – 12.227-010 – São José dos Campos – SP – Brazil

{marcos.rodrigues,thales.korting,gilberto.queiroz}@inpe.br

Abstract. *Water management is a field related to the increased mechanization of agriculture, mainly through center pivot irrigation systems, therefore it is important to identify and quantify these systems. Currently, with 6.95 million hectares, Brazil is among the 10 largest countries in irrigation areas in the world. In this study, a combined Computer Vision and Machine Learning approach is proposed for the identification of center pivots in remote sensing images. The methodology is based on Circular Hough Transform (CHT) to target detection and Balanced Random Forest (BRF) classifier using vegetation indices NDVI and SAVI generated from Landsat 8 and CBERS 4 images, being able to detect up to 90.48% of center pivots mapped by the Brazilian National Water Agency (ANA).*

1. Introduction

The practice of irrigation is one of the oldest techniques in agricultural production, used mainly by civilizations that developed in arid regions such as Egypt and Mesopotamia [Britannica Escola Web 2020]. Although agriculture initially developed predominantly in regions where the amount, spatial, and temporal distribution of rainfall was able to supply the need for crops. In Brazil the irrigation started around 1900 for rice production in the Rio Grande do Sul state. However, from the 1970 and 1980 decades, there was a significant intensification of agricultural activity in other regions. Leading to the rise of new irrigation poles according to the Brazilian National Water Agency (ANA) [ANA 2017].

Irrigation is an agricultural practice that employs a set of equipment and techniques to supply the total or partial deficiency of water for cultivation. On the one hand, the use of irrigation has several advantages for agricultural production, such as for example, increased productivity in relation to rainfed cultivation[1]. On the other hand, this use changes the availability conditions of water, because the water consumed by the evapotranspiration of plants and soil, not return to water bodies. Currently, with 6.95 million hectares, Brazil is among the 10 largest countries in irrigation areas in the world. However, the country still has great potential to be explored, according to ANA until the year 2030 there will be a strong expansion of the irrigation activity, especially by center pivot systems (Figure 1). The center pivot system is a mechanism formed by a galvanized

[1]Comparative of the productivity of rainfed and irrigated crops, source Secretariat of Water Resources of the Ministry of Environment SRH/MMA available on `https://www.codevasf.gov.br/linhas-de-negocio/irrigacao/a-irrigacao-no-brasil/comparativo`. Accessed on August, 24, 2020.

steel pipe suspended by towers with wheels at the base having water emitters along their length. This type of system irrigates a circular area by rotating this structure around a fixed point, called a pivot point, which serves to anchor the system and extract the water [Maranha 2018].

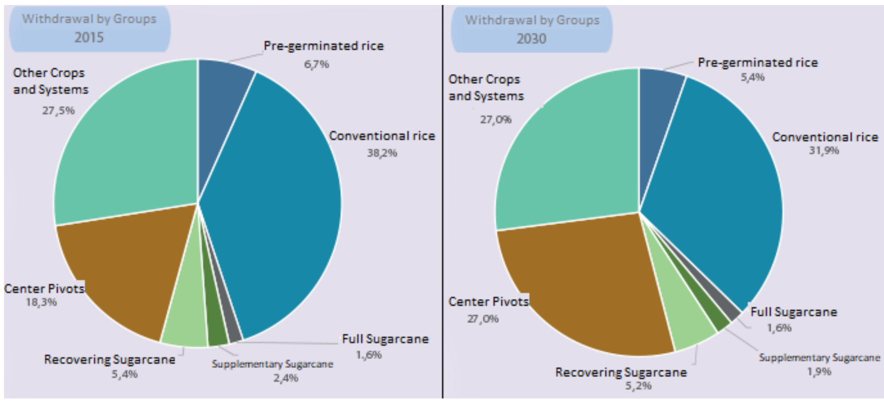

Figure 1. Water withdrawal by crop types and irrigation systems in 2015 and prevision for 2030. Adapted from ANA [2017].

In the literature review for this work, it was evident that in the vast majority of studies the remote sensing data is used only as a support tool associated with statistical data from official surveys or measures in situ [Maranha 2018], mainly in the visual analysis of satellite images for the mapping of irrigation pivot circles. According to Zhang et al. [2018], although the visual analysis of images is relatively simple, the identification and digitizing for a wide range of areas can be very time and labor consuming. Nowadays, with the advent of very high-resolution images and the increasing use of Machine Learning (ML) techniques, the use of automatic and semi-automatic techniques for the identification and classification of fields with irrigation crops has increased [Aksoy et al. 2012]. However, most approaches are limited to small areas of study (partial scene) and specific periods of the year. For example, Santos et al. [2015], present an approach to characterize areas irrigated by center pivots, based on the adjustment of vegetation response thresholds using the Normalized Difference Vegetation Index (NDVI) and Soil Adjusted Vegetation Index (SAVI) for two periods, rainy and dry, in an irrigated area of the municipality of Paranapanema-SP. This type of extremely localized approach does not allow the reproducible and generalization of the application of this methodology to other areas and regions, so much so that the values found by the authors differ from other study proposed for Demarchi et al. [2011] with the same type of approach to other regions and dates.

Based on the aforementioned considerations, this paper proposes a novel approach based on multistage processing to locating and quantifying center pivot irrigation systems based on target detection using Circular Hough Transform (CHT) over images of widely used spectral vegetation indices: NDVI and SAVI. Multistage involves the application of post-processing steps for handling errors that increase the false positive cases during the process of detecting circles by CHT. The main problems are false pivots detection in Riparian woods areas, urban areas and vegetated fields not irrigated by pivots.

2. Material and Methods

2.1. Study Areas

The main goal of this study is to identify a method ready to use in multisource remote sensing images. For this reason, we have chosen the scene of CBERS 4-Multispectral Camera (MUX) at path/row 164/117, this image has an important indigenous reserve of the Xavánte's, Sangradouro-Volta Grande in Mato Grosso state, Brazil, surrounded by a natural forest reserve. The scene also has a large number of agricultural fields employing center pivots. The second area of study is the region of city Paracatu in Minas Gerais state, according ANA and Embrapa [2019], this is one of the three main irrigating municipalities of Brazil in 2017, together with Unaí, also in Minas Gerais state; and Cristalina in Goiás state. These three cities form the highest concentration of pivots in Brazil with 2558 units occupying 191 thousand hectares, for this second area the Landsat 8-Operational Land Imager (OLI) scene at path/row 220/072 was analyzed (Figure 2).

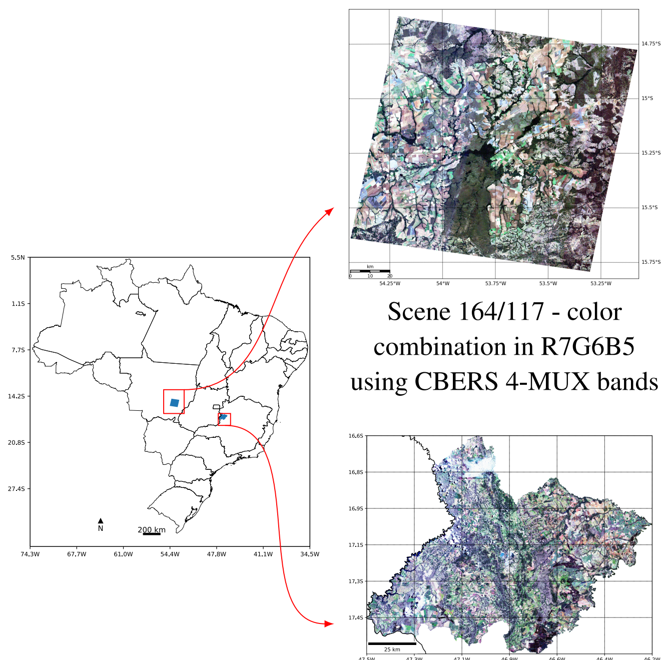

Scene 164/117 - color combination in R7G6B5 using CBERS 4-MUX bands

Detail of Paracatu-MG scene 220/072 - color combination in R4G3B2 using Landsat 8-OLI bands

Figure 2. Study areas using CBERS 4 and Landsat 8.

2.2. Data

The scene of Landsat 8-OLI covering Paracatu region was acquired for the year 2014 using the Google Earth Engine's (GEE) application programming interface, because this platform enables easy access to a product of surface reflectance from radiance measured by sensor, the process involves a detailed radiometric correction of solar energy scattered and reflected from the atmosphere and earth surface processed using algorithms supplied by U.S. Geological Survey. The GEE is a freely accessible, cloud-based platform designed to enable remote sensing studies over long time scales and large spatial extents [Gorelick et al. 2017]. The surface reflectance product from CBERS 4-MUX for the year 2017 was downloaded from the repository provided by Martins et al. [2018], which makes available the product of the images processed using Coupled Moderate Products for Atmospheric Correction (CMPAC) approach. The CMPAC uses atmospheric products from Moderate-Resolution Imaging Spectroradiometer (MODIS) and Visible Infrared Imaging Radiometer Suite (VIIRS) for atmospheric correction of CBERS 4-MUX level-4 images.

One of the post-processing stages involves the use of information over water bodies presence to eliminate false circles of pivots, to decrease the False Alarm Ratio (FAR), for this task we used Water Bodies for Brazil From RapidEye Images [Namikawa et al. 2016]. This mapping of water bodies has a pixel size of 5 m and use an approach based on the thresholding of the Hue component of the conversion of the color system from RGB to Hue-Saturation-Value (HSV), which has better results when compared to single-band thresholding or the use of Normalized Difference Water Index [Namikawa et al. 2016]. The results were organized in tiles with 125 km$\times$125 km in eight bits image having values from 1 to 7 to indicate the confidence of being a water pixel, from 1 as more confident to 7 as the less confident. The tiles can be downloaded using project interface[2], for our work the tiles 451, 452, 482, 483, 508, 509, and 510 needed for covering the Landsat scene, and tiles 301, 302, and 340 for covering CBERS scene.

The detection of center pivots was developed using remote sensing data from the years 2014/2017 and the geospatial vector dataset of center pivots mapped from ANA[3] in collaboration with Brazilian Agricultural Research Corporation (Embrapa) for the same years to validate results. This mapping was performed through visual analysis of Landsat, Sentinel, and other satellite images [ANA and Embrapa 2019].

2.3. Circular Hough Transform (CHT)

Duda and Hart [1972], present an approach to improve line and curve detection on digital images derived from the idea of parameter space or Hough Space (HS) originally defined by the parametric representation used to describe lines in the picture plane using Hough Transform (HT) [Hough 1962]. According to the authors, the general approach of the Hough Method can be extended to detect circular configurations (CHT), using a parametric representation for the family of all circles inside a region determined with maximum distance in the relation to the origin of parametric space. This way each figure point will be transformed into a circular cone in a three-dimensional parameter space represented for a 3D accumulator array, where the number of intersections between cones surfaces (votes) determines the centroids of geometric circles [Duda and Hart 1972]. The CHT

[2]Water Bodies for Brazil From the RapidEye Images repository, provided by Namikawa et al. [2016]. Available online: http://www.dpi.inpe.br/waterbodies/files/2014_2015_v3/download_wb_2015v3.php. Accessed on August, 25, 2020.

[3]GeoNetwork is the online repository of geospatial data made by ANA. Please refer to this address https://metadados.ana.gov.br/geonetwork/srv/pt/main.home?uuid=e2d38e3f-5e62-41ad-87ab-990490841073 to take access of geospatial vector dataset of center pivots. Accessed on January, 22, 2020.

is a simple feature extraction technique widely used in digital image processing for detecting circles in low-quality images, because of its robustness in the presence of noise, occlusion, and varying illumination [Dembele 2015].

We use the CHT method implemented in the OpenCV python library (The 2-1 Hough Transform - 21HT). It uses the gradient information of edges to decompose the circle finding problem into two stages, reducing the requirements of storage. The combining of CHT and vegetation indices, enable detect circular targets with the high response of vegetation indicating the health of the crop due to the use of center pivot irrigation systems.

2.4. Vegetation Indexes

Our approach used a pair of vegetation indexes to characterize vegetation density and enable detect crop fields irrigated of center pivot with high values of vegetation index. According Yin et al. [2012], NDVI can be explored for monitoring agricultural yield, using vegetation properties, such as length of the growing season, the onset date of greenness, and date of maximum photosynthetic activity. This way, Remote Sensing-based measurement is widely used to obtain phenological data in order to emphasize characteristics of terrestrial ecosystems to identify land cover and natural or anthropogenic changes.

Although the NDVI has been found highly correlated with vegetation parameters, some factors, such as atmospheric influences and soil substrate differences, impact the response obtained with him. Atmospheric turbidity generally inhibits reliable measures of vegetation and may delay the detection of the onset of stress in canopies such as green leaf area, biomass, percent green cover, productivity, and photosynthetic activity [Huete 1988]. For this reason, it is very important to combine NDVI with information from other indices, to analyze the behavior of vegetation response more carefully.

The SAVI was developed to enable correction to the response of partial energy reflected from soil surface exposed when the vegetative cover is low:

$$SAVI = \frac{NIR - RED}{NIR + RED + L} \times (1 + L), \tag{1}$$

where NIR is the reflectance value of the near infrared band, RED is reflectance of the red band, and L correction factor adjusts the original equation of NDVI to correct the soil brightness. The L value varies conform the presence of vegetation, very high ($L = 0$) to no vegetation ($L = 1$), but in most cases $L = 0.5$ is ideal to minimize soil brightness variations and eliminate the need for additional calibration for different soils [Huete 1988]. We adopted $L = 0.5$ to generate our SAVI images used to edge detection and extracting stats for detected circles.

2.5. Balanced Random Forest (BRF) For Pivot Identification

Our methodology described in Figure 3, shows the steps necessary to retrieve candidate circles of center pivot (x, y, radius), label the stats extracted from candidates circles, classify using BRF, and save pivots identified to compare with our knowledge database from ANA.

The major work consists of the following steps: (i) Apply the CHT technique over Canny edge detection results from vegetation index images (NDVI/SAVI) to identify

Figure 3. The framework for identification of center pivots using CHT and Balanced Random Forest Classification.

possible circles of the center pivots; (ii) Extract statistics from these circles, these samples of information was be labeled in pivot/not pivot through the spatial intersection of these circles with the pivots mapped by ANA; (iii) Fit a BRF model with labeled data to filter false alarm circles of pivots; (iv) Finally, validate filtered circles with ANA information.

Generally, pivot shape and vegetation index values vary significantly between different center pivot systems as a result of the variation of cultivation and irrigation. Our method is sensitive to the shape of the targets that are delimited using the Canny algorithm. Therefore, we decided to evaluate only those circles that had an average NDVI > 0.5. This made it possible to identify areas with the greatest photosynthetic activity, improving the delimitation of crop fields, and allowing better identification of center pivots.

2.5.1. Training Data

For each image processed, a set of circles is generated (Table 1). Each candidate circle is then examined to identify in its delimitation area the mean value and standard deviation of the vegetation indices, pixels of water bodies, edge pixels, and percentage difference of points (Figure 4). This information corresponds to the percentage difference between all points (edge pixels) included in the circle and points that form the convex hull of these points. This ratio is a good indicator of false detection of circles in cases where the analyzed object has many internal pixels.

Table 1. Candidates circles of pivots generated by CHT.

	NDVI	SAVI
Landsat 8	3856	11874
CBERS 4	1741	3083

All information generated during the analysis of circles builds a data set that after being labeled serves as input to train the classification model. As a result after classification, all the samples (circles) which received a positive indication of pivot are saved on geojson file to validate with pivots mapped by ANA.

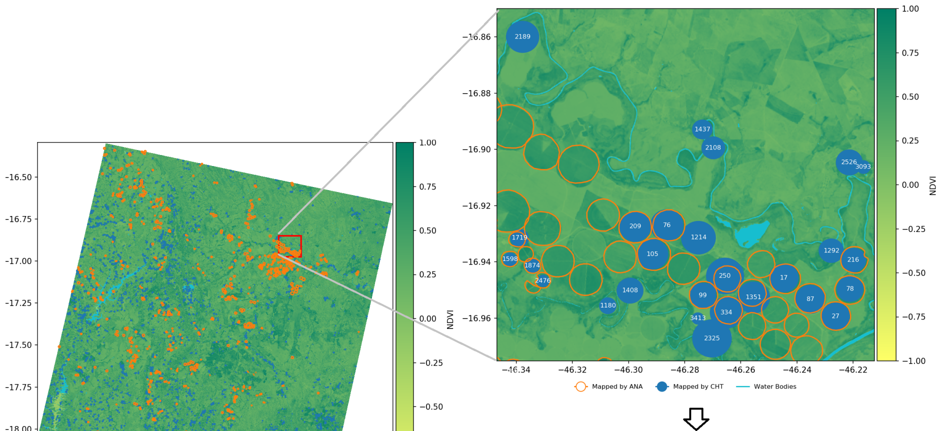

id	radius	DifPoints(%)	WaterPixels	Mean_ndvi	Std_ndvi	Mean_savi	Std_savi	PixelsWithin
17.0	19.0	83.58	0.0	0.67	0.11	0.45	0.09	16.0
27.0	18.0	81.82	0.0	0.65	0.12	0.43	0.08	0.0
76.0	21.0	87.25	0.0	0.61	0.14	0.41	0.1	0.0
78.0	17.0	77.42	0.0	0.65	0.09	0.45	0.06	0.0
87.0	19.0	84.62	0.0	0.61	0.15	0.39	0.09	0.0
99.0	17.0	80.65	0.0	0.7	0.17	0.49	0.12	0.0
105.0	20.0	78.81	0.0	0.6	0.11	0.39	0.07	0.0
176.0	14.0	78.26	0.0	0.52	0.12	0.38	0.09	0.0
209.0	20.0	84.21	0.0	0.59	0.12	0.38	0.08	0.0
216.0	16.0	82.61	0.0	0.66	0.1	0.45	0.07	0.0
250.0	24.0	94.46	0.0	0.57	0.2	0.39	0.15	59.0
334.0	21.0	89.35	27.0	0.61	0.17	0.38	0.12	23.0
349.0	14.0	82.08	0.0	0.62	0.14	0.45	0.11	0.0
1180.0	11.0	73.85	51.0	0.41	0.15	0.25	0.06	0.0
1214.0	22.0	73.58	0.0	0.32	0.08	0.22	0.05	0.0
1292.0	16.0	94.55	331.0	0.47	0.2	0.27	0.12	69.0
1351.0	21.0	82.93	0.0	0.55	0.11	0.36	0.07	0.0
1408.0	17.0	87.18	135.0	0.48	0.18	0.27	0.08	31.0
1437.0	13.0	89.26	217.0	0.53	0.19	0.27	0.1	10.0
1598.0	9.0	76.06	0.0	0.55	0.11	0.35	0.07	0.0
1719.0	12.0	85.58	0.0	0.61	0.14	0.4	0.1	13.0
1874.0	10.0	76.32	0.0	0.56	0.13	0.37	0.09	6.0
2108.0	15.0	90.54	181.0	0.4	0.16	0.23	0.07	33.0
2189.0	21.0	89.39	135.0	0.35	0.16	0.24	0.06	52.0
2325.0	25.0	91.84	373.0	0.51	0.13	0.26	0.08	117.0
2476.0	8.0	71.11	0.0	0.57	0.15	0.37	0.09	0.0
2526.0	17.0	89.29	34.0	0.35	0.14	0.21	0.07	16.0
3093.0	9.0	79.69	12.0	0.49	0.16	0.28	0.08	0.0
3413.0	8.0	73.68	0.0	0.27	0.13	0.17	0.06	0.0

Figure 4. Illustration of the stats information extraction from circles detected by CHT.

2.5.2. Data Analysis

The data analysis and processing were carried out using Python programming language due to the facilities provided by their libraries and packages. For instance, the Pandas and GeoPandas libraries were used to manage stats information of circles identified in images through CHT and label this information through intersects of pivots mapped by ANA [GeoPandas Development Team 2019].

Another important package used was Scikit-learn [Pedregosa et al. 2011], which includes a useful set of methods for the construction and evaluation of ML methods, such as Random Forest. However, as the problem we are deal with is characterized by unbalanced classes, it was necessary to use techniques to care with this imbalance. Because the learning and prediction of ML models are usually affected by the imbalance problem of a data set [Lemaître et al. 2017]. The balancing issue corresponds to the difference of the number of samples in the different classes, for example, the samples generated in the processing of the Landsat SAVI image, only 850 (7.16%) corresponded to pivots, of which 444 had mean NDVI > 0.5.

We employed two techniques to handle the problem of unbalanced classes, Random Over Sampler (ROS) and a classifier including inner balancing samplers (BRF), both were implemented in the imbalanced-learn package [Lemaître et al. 2017]. ROS uses a naive strategy to generate new samples of data set by randomly sampling with replacement of the currently available samples (Upsampling). While BRF is an ensemble method in which each tree of the forest will provide a balanced bootstrap sample [Chen et al. 2004]. These methods combined increased considerably the accuracy of the model (Figure 5) and consequently the result of the classification and filtering of the pivots.

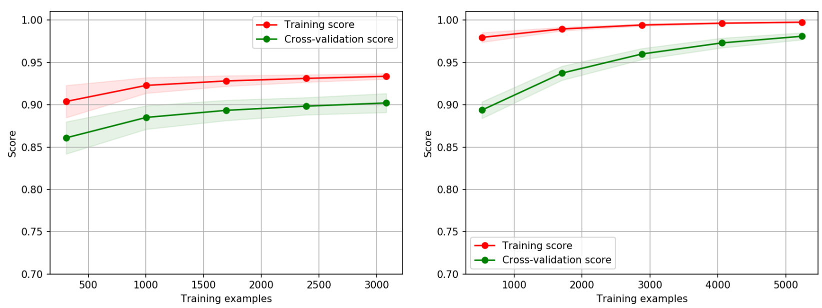

(a) Without Upsampling (b) With Upsampling

Figure 5. Learning results for BRF varying the number of training samples.

Processing was performed on a machine with 8 cores and 8 GB of memory. Training and predict with the BRF model took a few seconds because the data set is small (maximum 11874 samples). However, the iterative process for extracting statistics for each circle identified by the CHT method reached the time of 132 min. But using the multiprocessing module for Python which allowed us to reduce that time to 1/4 by executing the extraction function in multiple processes occupying all cores at the same time.

3. Results

As previously presented, the BRF model achieved high accuracy for classifying the pivots. In this manner, we have the maximum Recall limited by the CHT method and the FAR minimized by the classification provided by the BRF. Basically, Recall means how much of the total of pivots are in this area the method can be recover, and FAR how much of the total pivots identified by BRF not match with pivots mapped in this area by ANA. It is important to mention that the CHT method can generate the identification of overlapping circles (Overlapping Identifications) because there is a trade-off between the necessity to detect small and large circles of pivots (400 to 1000 m).

Figure 6 present the results achieved for the CBERS scene, the blue-dots represent pivots correctly identified by our approach, red-dots false alarm of pivots and orange-dots pivots not identified. This result, emphasizes that the method is optimal to filters circles of not pivot, but the capacity to recover all pivots depends on a variety of characteristics linked to the vegetative response of the targets that depend on agricultural production cycles.

To quantify and analyze the results on this scene, we compare the number of pivots mapped by ANA in this testing area. The Recall and FAR of identification were calculated with data in Table 2. They show that in this area there are 84 pivots mapped by ANA with (Mean NDVI > 0.5), while our approach was able to identify 66 pivots all matching with pivots of ANA, but exist one overlapped detection, this manner based on the NDVI image we achieved a Recall of 77.38% and FAR of 0%. When the image used is SAVI, we identified 88 pivots, but among them, three no match with ANA and

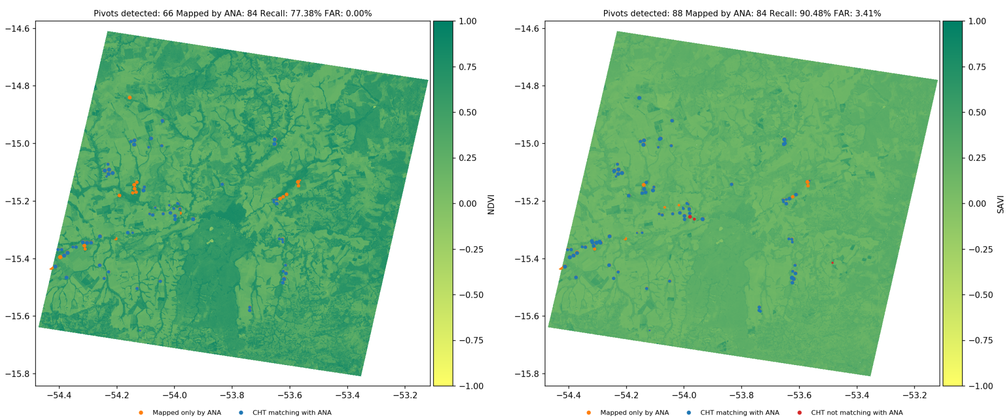

(a) NDVI

(b) SAVI

Figure 6. Blue-dots represent pivots correctly identified, red-dots false alarm of pivots and orange-dots pivots not identified. Pivots identification based on vegetation images of scene CBERS 4 path/row 164/117 in July 2017.

nine overlaps achieving a Recall of 90.48% and FAR of 3.41%. This proves that although the detection with the SAVI image generates a higher processing volume, more circles not corresponding to pivots, it allows a greater recall thus enhancing its advantage over NDVI, due to the brightness adjustment factor for exposed soil.

Table 2. Quantity analysis results for CBERS scene.

	Mapped by ANA	Pivots Identified	Overlapping Identifications	Match ANA	Not Match ANA
Count by NDVI	84	66	1	65	0
Count by SAVI	84	88	9	76	3

For further analysis of the Paracatu-MG region, we needed before process the scene of Landsat 8 path/row 220/072. For this reason, we decided to show the results achieved for both, the entire scene and clipping to the region (Figures 7 and 8). The parameters of the classifier are tuned for each type scene and satellite, we believe that this process should guarantee the best result taking into account the intrinsic differences between the spectral responses recorded by each sensor (satellite) and by each type of image (vegetation indexes) regardless of the chosen date and geographical position.

Table 3, compiles both the information for the entire scene and the clipping region. For this area, ANA mapped 609 pivots with (Mean NDVI > 0.5) for the entire scene and 262 for Paracatu-MG region, while our approach identified 444 and 193 pivots respectively all matching with pivots of ANA, but with seven/two overlaps. Therefore, based on NDVI image we achieved a Recall of 71.76% and 72.90% respectively, and FAR of 0% for both. When the image used is SAVI, we identified 492 pivots for the scene and 205 pivots for clipping all matching with pivots of ANA, but there are 16/3 overlaps, resulting in Recall of 78.16% and 77.10% and FAR of 0%. Once again the response with the SAVI image was better. Although for this scene the Recall had lower values than about the other satellite (CBERS), this is possibly linked to the condition of vegetation in this date and agricultural calendar of this region.

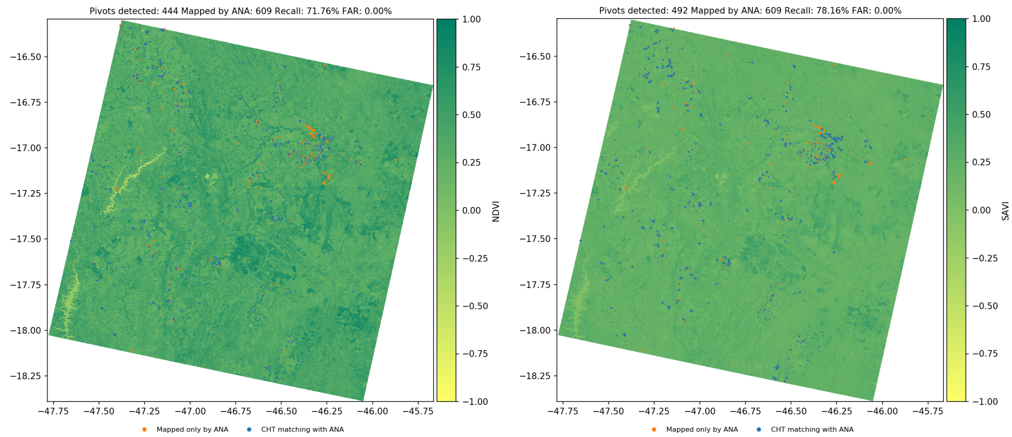

(a) NDVI (b) SAVI

Figure 7. Pivots identification based on vegetation images of scene Landsat 8 path/row 220/072 in August 2014.

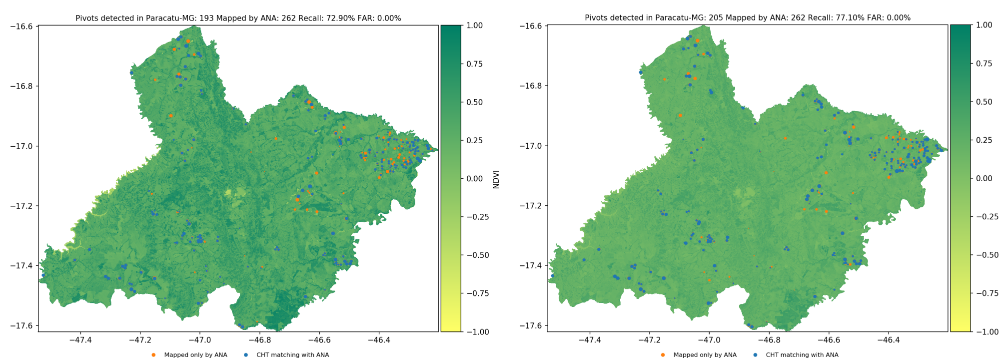

(a) NDVI (b) SAVI

Figure 8. Pivots identification (Paracatu-MG region) based on vegetation images of scene Landsat 8 path/row 220/072 in August 2014.

4. Conclusion

The aim of this study was to automatically identify center pivots on multisource remote sensing images using image processing techniques and ML models. The proposed approach identified pivots successfully using the BRF model trained with different types of stats extracted of targets detected by CHT over scenes from Landsat 8 and CBERS 4. The high accuracy achieved shows the robustness of the method and data independence. The results were validated with mapping carried out by ANA, presenting less economic cost and less time than a visual analysis approach. Several factors can negatively influence our results, such as the highest presence of clouds and shadow. Besides that, urban areas and water bodies can result in high levels of false positives, due to a large number of edge pixels generated in these regions, but this problem was handled with success using the Random Over Upsampling technique and Balanced Random Forest classifier to filter not pivot circles in this areas. As future work, we plan to use a collection of a year images to identify the greenest pixels (maximum NDVI), this would allow improving the

Table 3. Quantity analysis results for Landsat scene an Paracatu-MG region.

	Mapped by ANA Scene/Clipping	Pivots Identified Scene/Clipping	Overlapping Identifications Scene/Clipping	Match ANA Scene/Clipping
Count by NDVI	609/262	444/193	7/2	444/193
Count by SAVI	609/262	492/205	16/3	492/205

***Attention** - this table does not have collumn "Not Match ANA" because for both areas the FAR values are null.

delimitation of pivots by the Canny algorithm. In addition, we also intend to adopt an approach based on time series similar to that used by Rodrigues et al. [2020], who used them to adjust thresholds for identifying pivots in the MATOPIBA region. However, our goal is to use the time series classification obtained from the detected targets in order to characterize the region based on land use and crop cycles.

Acknowledgements

This study was supported in part by grants 2017/24086-2 and 2018/16221-0, São Paulo Research Foundation (FAPESP), the Coordenação de Aperfeiçoamento de Pessoal de Nível Superior - Brasil (CAPES) - Finance Code 001 and the Brazilian National Council for Scientific and Technological Development (CNPq, grant 303360/2019-4). Also, we thank the National Institute for Space Research and the subproject Brazil Data Cube, of the Environmental Monitoring Project for Brazilian Biomes, financed by the Amazon Fund, through the financial collaboration BNDES and FUNCATE nº 17.2.0536.1.

References

Aksoy, S., Yalniz, I. Z., and Tasdemir, K. (2012). Automatic detection and segmentation of orchards using very high resolution imagery. *IEEE Transactions on geoscience and remote sensing*, 50(8):3117–3131.

ANA (2017). Atlas irrigação: Uso da água na agricultura irrigada. Technical report, National Water Agency (ANA). arquivos.ana.gov.br/imprensa/publicacoes (10 May 2019).

ANA and Embrapa (2019). Levantamento da agricultura irrigada por pivôs centrais no Brasil (1985-2017). Technical report, National Water Agency (ANA) and Brazilian Agricultural Research Corporation (Embrapa) Maize/Sorghum. ana.gov.br (10 May 2019).

Britannica Escola Web (2020). Irrigação. In Britannica Escola. Web, escola.britannica.com.br/artigo/irrigação/481588 (18 October 2020).

Chen, C., Liaw, A., Breiman, L., et al. (2004). Using random forest to learn imbalanced data. Technical report, University of California, Berkeley. statistics.berkeley.edu (20 September 2020).

Demarchi, J. C., Piroli, E. L., and Zimback, C. R. L. (2011). Analise temporal do uso do solo e comparação entre os índices de vegetação ndvi e savi no município de santa cruz do rio pardo–sp usando imagens landsat-5. *Raega-O Espaço Geográfico em Análise*, 21.

Dembele, F. (2015). Object detection using Circular Hough Transform. Université Laval. wcours.gel.ulaval.ca/2015/a/GIF7002/default/5notes [Lectures supplémentaires C11:d] (25 January 2019).

Duda, R. O. and Hart, P. E. (1972). Use of the Hough transformation to detect lines and curves in pictures. *Communications of the ACM*, 15(1).

GeoPandas Development Team (2019). GeoPandas Library, Version 0.5.1. GeoPandas developers Revision 4a4ede8b. geopandas.readthedocs.io/en/v0.5.1 (27 August 2019).

Gorelick, N., Hancher, M., Dixon, M., Ilyushchenko, S., Thau, D., and Moore, R. (2017). Google earth engine: Planetary-scale geospatial analysis for everyone. *Remote Sensing of Environment*.

Hough, P. V. (1962). Method and means for recognizing complex patterns. US Patent 3,069,654.

Huete, A. (1988). A soil-adjusted vegetation index (savi). *Remote sensing of environment*, 25:295–309.

Lemaître, G., Nogueira, F., and Aridas, C. K. (2017). Imbalanced-learn: A python toolbox to tackle the curse of imbalanced datasets in machine learning. *Journal of Machine Learning Research*, 18(17):1–5.

Maranha, L. G. (2018). Mapeamento semiautomático de áreas irrigadas por pivôs centrais por meio de análise espacial orientada a objetos em imagem Landsat 8.

Martins, V. S., Soares, J. V., Novo, E. M., Barbosa, C. C., Pinto, C. T., Arcanjo, J. S., and Kaleita, A. (2018). Continental-scale surface reflectance product from cbers-4 mux data: Assessment of atmospheric correction method using coincident landsat observations. *Remote Sensing of Environment*, 218:55–68.

Namikawa, L. M., Körting, T. S., and Castejon, E. F. (2016). Water body extraction from rapideye images: An automated methodology based on hue component of color transformation from rgb to hsv model. *Revista Brasileira de Cartografia*, 68(6).

Pedregosa, F., Varoquaux, G., Gramfort, A., Michel, V., Thirion, B., Grisel, O., Blondel, M., Prettenhofer, P., Weiss, R., Dubourg, V., Vanderplas, J., Passos, A., Cournapeau, D., Brucher, M., Perrot, M., and Duchesnay, E. (2011). Scikit-learn: Machine learning in Python. *Journal of Machine Learning Research*, 12:2825–2830.

Rodrigues, M. L., Körting, T. S., de Queiroz, G. R., Sales, C. P., and d. Silva, L. A. R. (2020). Detecting center pivots in Matopiba using hough transform and web time series service. In *2020 IEEE Latin American GRSS ISPRS Remote Sensing Conference (LAGIRS)*, pages 189–194.

Santos, J. É. O., Nicolete, D. A. P., Filgueiras, R., Leda, V. C., and Zimback, C. R. L. (2015). Imagens do Landsat-8 no mapeamento de superfícies em área irrigada. *Irriga, Edição Especial, IRRIGA & INOVAGRI*, pages 30–36.

Yin, H., Udelhoven, T., Fensholt, R., Pflugmacher, D., and Hostert, P. (2012). How Normalized Difference Vegetation Index (NDVI) Trends from Advanced Very High Resolution Radiometer (AVHRR) and Système Probatoire d'Observation de la Terre VEGETATION (SPOT VGT) Time Series Differ in Agricultural Areas: An Inner Mongolian Case Study. *Remote Sensing*, 4(11):3364–3389.

Zhang, C., Yue, P., Di, L., and Wu, Z. (2018). Automatic identification of center pivot irrigation systems from landsat images using convolutional neural networks. *Agriculture*, 8(10):147.